Almost Compact Breathers in Anharmonic Lattices near the Continuum Limit

P. Rosenau* and S. Schochet†

School of Mathematical Sciences, Tel-Aviv University, Tel Aviv 69978, Israel

(Received 25 August 2004; published 3 February 2005)

Certain strictly anharmonic one-dimensional lattices support discrete breathers over a macroscopic localized domain that in the continuum limit becomes exactly compact. The discrete breather tails decay at a double-exponential rate, so such systems can store energy locally, especially since discrete breathers appear to be stable for amplitudes below a sharp stability threshold. The effective width of other solutions broadens over time, but, under appropriate conditions, only after a positive waiting time. The continuum limit of a planar hexagonal lattice also supports a compact breather.

DOI: 10.1103/PhysRevLett.94.045503 PACS numbers: 63.20.Pw, 63.20.Ry

A wide variety of physical systems are described by anharmonic lattices that on the macroscopic length scale involve many unit cells, and thus in a first approximation are modeled using the continuum limit described via partial differential equation(s) (PDE) with the discrete effects being completely washed away. Since the continuum limit is singular, and the resulting equations exhibit a number of surprising features, it is essential to understand the impact of discreteness on the overall dynamics. In this Letter we study a class of purely anharmonic lattices (the impact of harmonic interaction is discussed as well) and show that such systems support almost-compact breathers over a macroscopic domain. These energy-storing essentially nonlinear modes of vibration are of fundamental importance and of long-standing interest. Although, in principle, lattices governed by Newton's laws immediately spread any information presented over a compactum, we demonstrate that the effective spread is actually very limited and the continuum limit correctly predicts the essentially compact span of the breather. Beyond the breathers' support the discrete effects decay at a *doubly exponential rate.* Thus the purely anharmonic interparticle interaction, in addition to *nonlinear force and nonlinear dispersion,* creates a genuine screening effect beyond which there is no measurable motion. In this sense the effects to be presented differ in a fundamental way from classical solitons or breathers and the like. See [1] for an overview of these issues.

Equations and scaling.—Consider the Hamiltonian

$$H_{\text{disc}} = \sum_{n=-N}^{N} \frac{m\dot{y}_n^2}{2} + \ell\{P(\frac{y_{n+1} - y_n}{\ell}) + \Phi(y_n)\} \qquad (1)$$

describing a chain of $2N + 1$ particles of equal mass m and equal spatial separation ℓ, where P and Φ denote the interaction and site potentials, respectively. Fixing the total length $L = 2N\ell$ and density $\rho = m/\ell$ of the chain while letting $m \downarrow 0$ and $\ell \downarrow 0$, and hence $N \uparrow \infty$ yields the continuum limit

$$H_{\text{cont}} = \int \left\{ \frac{\rho y_t^2}{2} + P(y_x) + \Phi(y) \right\} dx. \qquad (2)$$

Henceforth we consider the potentials

$$P(S) = \frac{a}{4} S^4, \qquad \Phi(y) = \frac{b}{2} y^2 - \frac{c}{4} y^4 \quad \text{with } a, b > 0. \qquad (3)$$

All four parameters ρ, a, b, and c appearing in the equation of motion derived from H_{cont} can be eliminated up to the sign by rescaling t, x, and y, yielding an *anharmonic* Klein-Gordon equation (aKG)

$$y_{tt} + y = \frac{\partial}{\partial x}(y_x)^3 + \text{sgn}(c) y^3, \qquad (4)$$

since ρ, a, and b are positive on physical grounds. That spatial gradients are nonlinear is a major change from the conventional Klein–sine-Gordon case for now; as is typical for quasilinear wave equations in general, second derivatives of solutions of the aKG may become infinite in a finite time (the mollifying effect of dispersion due to the site potential is in general ineffective in arresting the gradient catastrophe). It is the dispersion due to the discrete lattice which prevents this blowup, *hence its singular effect on the dynamics.* In normalized units, which are used throughout this Letter, the limiting period of small-amplitude oscillations is 2π and, as is shown shortly, the half length and the amplitude A of the stationary compacton are

$$L_0 = \frac{3^{1/4}\pi}{\sqrt{2}} \approx 2.92, \qquad A = \sqrt{2}. \qquad (5)$$

Similarly rescaling the discrete equations of motion arising from (1) yields the system

$$\ddot{y}_n + y_n = \frac{1}{h}\left[\left(\frac{y_{n+1} - y_n}{h} \right)^3 - \left(\frac{y_n - y_{n-1}}{h} \right)^3 \right] + \text{sgn}(c) y_n^3, \qquad (6)$$

where the nondimensional parameter $h = \ell(|c|/a)^{1/4}$ measures the distance from the continuum limit. Unlike the continuum model Eq. (4), small-amplitude solutions of (6) exist indefinitely.

Small-amplitude scaling.—In the low-amplitude regime, a scaling law relating time to amplitude emerges: writing

 © 2005 The American Physical Society

Eq. (4) in terms of $w = e^{it}(y + iy_t)$ yields an equation in standard averaging form [2], with the sum of squares of the initial amplitude and velocity playing the role of the small parameter. The averaged equation

$$w_t = \frac{3i}{8}\left\{\frac{\partial}{\partial x}[|w_x|^2 w_x] + \mathrm{sgn}(c)|w|^2 w\right\} \tag{7}$$

is invariant under $w \mapsto \alpha w$, $t \mapsto t/\alpha^2$. Note that this scaling law, which is consistent with the time scale of the validity of the averaging approximation and applies in the discrete case as well, concerns not the period of oscillations of y, but rather the slower motions that take place against that background. Unlike Eq. (4), Eq. (7) does not allow shocks.

Breathers.—We begin with Eq. (4). Since the nonlinearities there all involve the same power, separated solutions $y = \phi(t)\psi(x)$ exist (cf., e.g., [3]), with

$$\ddot{\phi} + \phi = \lambda\phi^3, \tag{8}$$

$$[(\psi')^3]' + \mathrm{sgn}(c)\psi^3 = \lambda\psi. \tag{9}$$

Multiplying (9) by ψ' and integrating yields

$$3(\psi')^4 - 2\lambda\psi^2 + (c)\psi^4 = E = \text{const.} \tag{10}$$

For compactly supported solutions *E must equal zero* since ψ and ψ' both vanish for large $|x|$. Such a ψ, not vanishing identically, has a nonzero spatial extremum, at which $\psi' = 0$, so λ and c must have the *same nonzero sign,* which must be positive for ψ to remain real for ψ near zero. Hence a nontrivial compact solution can exist *only when* $c > 0$. The separation constant λ may then be normalized to one by rescaling ϕ and ψ while leaving their product y unchanged, which reduces Eq. (10) to

$$3(\psi')^4 - 2\psi^2 + \psi^4 = 0. \tag{11}$$

This shows that ψ has amplitude $\sqrt{2}$ as stated in Eq. (5), while the normalized (8) shows that solutions y of smaller amplitude oscillate periodically and those of larger amplitude blow up. Solving (11) yields

$$|x| = \frac{3^{1/4}}{2}\left[\sqrt{2}\pi - B\left(\frac{\psi^2}{2}, \frac{1}{4}, \frac{3}{4}\right)\right], \tag{12}$$

where the incomplete beta function B is defined by

$$B(s, a, b) = \int_0^s u^{a-1}(1-u)^{b-1}du, \tag{13}$$

which imply that ψ vanishes at the value L_0 given in (5). Near $x = L_0$, $\psi \sim \frac{(x-L_0)^2}{2\sqrt{6}}$, which makes Eq. (9) degenerate there. This degeneracy allows us to continue the solution by zero for $|x| > L_0$, yielding a compact solution. Indeed, substituting the expansion $\psi \sim \frac{(x-L_0)^2}{2\sqrt{6}}H(x - L_0)$ with $H(x)$ being the Heaviside function into (9), we find that the most singular terms balance.

The above considerations show that for compactification to take place, not only a degeneracy of the spatial gradients (or amplitudes) is necessary, but also that they be balanced by the inertial force. A counterexample is afforded by the periodic solution $y = \theta(t)\cos(\beta x)$ of (4) for $c < 0$, which cannot be extended by zero outside the interval $|x| \le \frac{\pi}{2\beta}$ as proposed in [4]: Using $y \sim -\theta(t)(\beta x - \frac{\pi}{2})H(\beta x - \frac{\pi}{2})$ in (4), the spatial-derivative term yields a Dirac delta function not balanced by any other term, so the truncation is not a solution.

The long-time persistence of such small-amplitude truncated cosine profiles reported in [4] is not a special property of that shape but rather a consequence of the time-amplitude scaling law derived above: As shown in Figs. 1 and 2, the solution of Fig. 3(c) of Ref. [4], whose normalized amplitude is 0.01, does change shape after a time consistent with the time-amplitude scaling law, while the continuum breather, which is an approximation of the true discrete breather, still maintains its shape.

Almost-compact discrete breathers.—The separation ansatz $y_n = \phi(t)\psi_n$ is equally applicable to the discrete Eqs. (6) (cf., e.g., [5]), and leads to the normalization of (8) for ϕ plus

$$\frac{1}{h}\left[\left(\frac{\psi_{n+1} - \psi_n}{h}\right)^3 - \left(\frac{\psi_n - \psi_{n-1}}{h}\right)^3\right] + \psi_n^3 = \psi_n. \tag{14}$$

Equation (14) implies that if ψ_n equals zero but ψ_{n-1} does not, then ψ_{n+1} must also be nonzero, which shows that nonzero strictly compactly supported solutions cannot exist. In view of this impossibility, also noted in [5–7], the compactons proposed in [7,8] are not exact solutions.

In [9] we prove that (14) has two solutions that are perturbations of the continuum compacton. Although a number of existence results for exact discrete breathers have been obtained (see [10] for a review), they apply

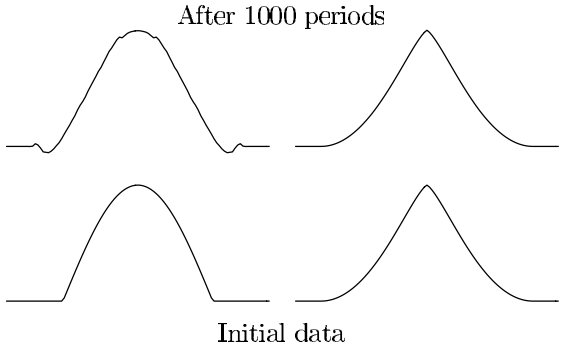

FIG. 1. The persistence of breathers: Solutions beginning with truncated cosine (left) and continuum breather (right) profiles of normalized amplitude 0.01, with $h = 0.0725$ and zero initial derivative. The lower curves shows the initial values, while the upper curves show the solutions after 1000 periods of oscillation. The truncated cosine solution differs from its initial profile by up to 7.8% of its amplitude, but the continuum breather solution differs by at most 0.15%.

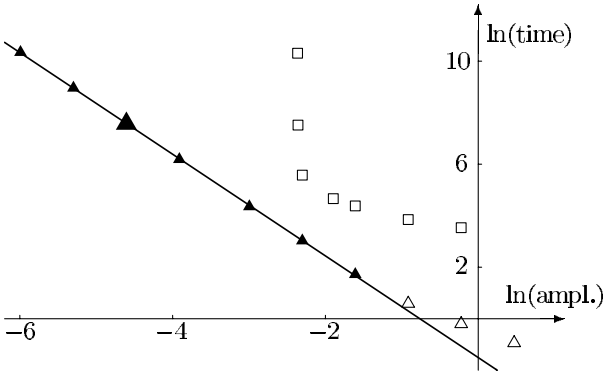

FIG. 2. The time-amplitude scaling: Log-log plots of amplitude vs the time at which the effective width of the solution increases by 0.3, for the truncated cosine profile (▲,△) and the continuum breather profile (□), with $h = 0.0725$ and zero initial derivative. The least-squares fit line for the truncated cosine profile, based only on ▲, has slope -1.97. The large triangle represents Fig. 1, confirming that that case is well represented by the time-amplitude scaling law. The anomalously large times obtained for the small-amplitude continuum breather illustrate the stability threshold discussed below.

either to the ''anticontinuum limit'' in which h is large [11], to special interaction potentials not applicable to chains governed by Newton's equations as considered here [12], to equations without site potentials or including linear interaction terms [13,14], or to solutions whose sign changes from each site to the next [15] (dimers) and so neither converge nor have finite energy in the continuum limit. We calculate the discrete breather profiles numerically by a one-parameter shooting method, with the other free parameter determined by the symmetry condition $\psi_1 = \psi_{-1}$ or $\psi_{1/2} = \psi_{-1/2}$.

Effects of discreteness.—While $\phi_n \approx \psi(nh)$ for $nh < L_0$, for $nh > L_0$ the discrete profile does not vanish identically like the continuum profile, but obeys the double-exponential decay law

$$\frac{\ln|\ln\psi_n|}{n} \to \ln 3. \tag{15}$$

The same result was obtained in [16] for large-h alternating-sign discrete breathers. Such faster-than-exponential decay on the fast x/h spatial scale is the defining property of almost-compact solutions.

Although the method of [17] could be used to develop a well-posed equation with leading dispersive effects imbedded, the equation so obtained is valid only away from the peak and the tails of the breather profile, because of the limited smoothness of the continuum profile near its peak and the decay on the fast x/h spatial scale of the discrete profile in the tails.

The limited smoothness of the continuum profile at its peak causes the discrete breather profile to differ not by the order h^2 expected for an even perturbation, but by $O(h^{4/3})$ [9]. Still, for the moderately small value $h = 0.0725$ used in the computations of Figs. 1 and 2, the maximum discrepancy between the discrete and continuum profiles is only 0.1% of the breathers' amplitude, Even for $h = 0.4$, the deviation between the discrete and continuum profiles is only 2% of the amplitude; see Fig. 3. *In particular, the effective width of the discrete breather is essentially the same as that of the continuum breather, independently of the number of cells within that width.*

Stability.—Although the discrete breather, being an exact solution of Eq. (6), retains its shape indefinitely, its actual importance depends on the degree of its stability. Since Eq. (6) is a Hamiltonian, at best neutral stability might hold. Calculations indicate the existence of a sharp h-dependent amplitude threshold, below which the discrete breather is indeed stable. This threshold can be seen clearly in Fig. 2, where a 1% decrease in amplitude of the continuum breather caused a 70-fold increase in time needed for the edge of the solution to move a fixed amount 0.3. A more traditional measure of stability is the rate of increase of the size of a small random perturbation, say, initially restricted to the support of the continuum breather. Calculations using the same value $h = 0.0725$ show that for amplitude 0.1 the size of such perturbations of the discrete breather increases 100-fold within 10 periods of oscillation, but for amplitude 0.09 the same perturbations merely fluctuate in size within a range from 0.7 to 1.5 times their initial amplitude throughout more than 500 oscillations.

A related issue is that of perturbations due to mechanisms not included in our model, with the harmonic force being the uppermost example. In the case of a sparse lattice wherein the system has an extended domain of stability, a small harmonic part causes a minor amplitude change and a very slow leakage of the breather's support, which raises the tails. The following numbers are typical: for a normalized coefficient of the harmonic force $= 10^{-4}$ which in actual units is not too small, and $h = 1/4$, after 500 *oscillations* the breathers amplitude has changed by less

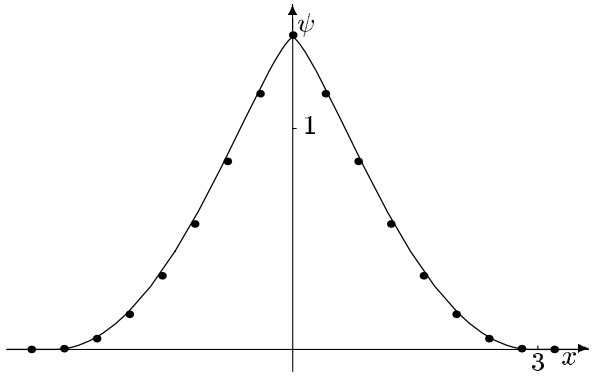

FIG. 3. Comparison of continuous (line) and sparse discrete (dots) breather profiles for $h = 0.4$.

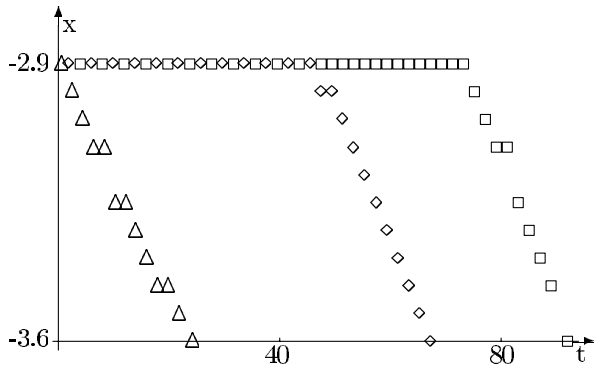

FIG. 4. The waiting-time phenomenon: Effective edge of support as a function of time for solutions beginning with truncated cos (△), truncated $\cos^4$ (◇), and continuum breather (□) profiles, all scaled to amplitude 0.2 and half length L_0. The edge of the linear-edged cos profile begins to move immediately, but the edge of the superlinear profiles stays put for a while. The edge is defined as the point where the root mean square of the solution and its derivative first exceeds a tolerance equal to half the smallest nonzero value of the initial data. Lowering this tolerance by a factor of 10^{-12} moves the edge by at most three grid points for the linear-edged profile and at most two grid points for the other cases.

then 0.02, and four mass points ($x \sim 4$) beyond the exact boundary (~ 2.92) the amplitude is now $\sim 10^{-4}$. Thus the harmonic perturbation turns a permanent pattern into a very long one.

The waiting-time effect.—The loss of localization, as measured by the spreading of the support of the solution, provides a physically meaningful measure of the change of shape of a solution. Although discrete solutions do not have strictly compact support, when their initial data have compact support then their tails decay exceedingly rapidly, in a similar fashion to the discrete breather profile. This makes the effective support fairly insensitive to exactly how it is defined, as described in Fig. 4. That figure also illustrates the fact that the permanent localization of the exact breather is but the extreme case of the *waiting-time phenomenon* before spreading begins. This occurs when the initial profile is superlinear at its edge, since the vanishing of y_x there makes the wave speeds $C \sim y_x$ of the continuum equation become degenerate. In a linear problem where $C(x)$ is predetermined, that would mean a permanent trap; in our case there is a finite-time wait during which the solution reshapes at the edge. This "opens the gate," and the wave spreads out of its initial support. In the frame of the PDE equation, the spreading of the support requires the formation of energy-dissipating shocks, while the original ordinary differential equation chain preserves energy for all time. The dense chain used in the computation of Fig. 4 is close to the continuum; as h increases two effects occur concurrently: notably, the waiting time increases, and simultaneously its sensitivity on the choice of initial pulse decreases, since there are fewer cells to distinguish between different shapes.

A planar compact breather.—Rectangular planar anharmonic lattices lead to anisotropic continuum models [17]. To ensure that nearest-neighbor interactions with quartic potentials like (3) yield an isotropic continuum, we use a hexagonal lattice to obtain

$$Z_{tt} + Z = \nabla \cdot [|\nabla Z|^2 \nabla Z] + Z^3, \tag{16}$$

where the equation has been normalized as above [17]. Averaging out the quick oscillations, as in 1D, we derive a 2D variant of Eq. (7) and similar conclusions regarding the scaling of the amplitude with time. Equation (16) admits separated radial solutions $Z = \phi(t)\psi(|x|)$. Although the nonlinear equation determining the shape of ψ can no longer be integrated explicitly, a compact solution having a similar shape to its 1D cousin exists [9]. Since compactness is caused by the degeneracy of the highest-order operator, which is independent of dimension, compactness persists in all dimensions and, indeed, occurs in a variety of different processes like thermal waves in plasma. As ϕ still satisfies (8), breathers are once again obtained for amplitudes below that of the stationary compacton.

In summary, we have unfolded an almost-compact, robust, macroscopic discrete breather which remains intact in the continuum limit in one and two dimensions, where it becomes exactly compact.

*Electronic address: rosenau@post.tau.ac.il
†Electronic address: schochet@post.tau.ac.il

[1] D. Campbell, S. Flach, and Y. Kivshar, Phys. Today **57**, No. 1, 43 (2004).
[2] J. A. Sanders and F. Verhulst, *Averaging Methods in Nonlinear Dynamical Systems* (Springer-Verlag, Berlin, 1985).
[3] P. Rosenau, Phys. Rev. Lett. **73**, 1737 (1994).
[4] P. T. Dinda and M. Remoissenet, Phys. Rev. E **60**, 6218 (1999).
[5] S. Flach, Phys. Rev. E **50**, 3134 (1994).
[6] P. G. Kevrekidis, V. V. Konotop, and S. Takeno, Phys. Lett. A **299**, 166 (2002).
[7] J. C. Comte, Phys. Rev. E **65**, 067601 (2002).
[8] Y. Kivshar, Phys. Rev. E **48**, R43 (1993).
[9] P. Rosenau and S. Schochet (to be published).
[10] S. Flach and C. R. Willis, Phys. Rep. **295**, 181 (1998).
[11] R. S. MacKay and S. Aubry, Nonlinearity **7**, 1623 (1994).
[12] P. G. Kevrekidis, V. V. Konotop, A. R. Bishop, and S. Takeno, J. Phys. A **35**, L641 (2002).
[13] G. James, C. R. Acad. Sci. Ser. I Math. **332**, 581 (2001).
[14] S. Aubry, G. Kopidakis, and V. Kadelburg, Discrete Cont. Dynam. Syst. Ser. B **1**, 271 (2001).
[15] S. Flach, Phys. Rev. E **51**, 1503 (1995).
[16] B. Dey, M. Eleftheriou, S. Flach, and G. P. Tsironis, Phys. Rev. E **65**, 017601 (2001).
[17] P. Rosenau, Phys. Lett. A **311**, 39 (2003).